Stenoparib, an inhibitor of cellular poly (ADP-ribose) polymerases (PARPs), blocks *in vitro* replication of SARS-CoV-2 variants

Katherine E. Zarn[a]*, Sierra A. Jaramillo[a]*, Anthony R. Zapata[a], Nathan E. Stone[a], Ashley Jones[a], Haley Nunnally[a], Erik W. Settles[ab], Ken Ng[a], Paul Keim[ab], Steen Knudsen[c], Patricia Nuijten[d], Aloys Tijsma[d], Christopher T. French[ab]#.

[a]Pathogen and Microbiome Institute, Northern Arizona University, Flagstaff, AZ 86011-4073

[b]Department of Biological Sciences, Northern Arizona University, Flagstaff, AZ 86011-5640

[c]Allarity Therapeutics, DK-2970 Hørsholm, Denmark

[d]Viroclinics-DDL, Rotterdam, The Netherlands

Running Head: Stenoparib inhibits SARS-CoV-2 variants *in vitro.*

*These authors contributed equally to the study.

#Address correspondence to Christopher T. French, ctfrench@nau.edu

Keywords

COVID-19, antiviral, SARS-CoV-2, coronavirus, stenoparib, remdesivir

Abstract

We recently published a preliminary assessment of the activity of a poly (ADP-ribose) polymerase (PARP) inhibitor, stenoparib, also known as 2X-121, which inhibits viral replication by affecting pathways of the host. Stenoparib is an inhibitor of mammalian poly (ADP-ribose) polymerases (PARPs). Here we show that stenoparib effectively inhibits additional SARS-CoV-2 variants, including an additional wild-type strain (Germany/BavPat1/2020), and the variants *alpha* (B.1.1.7), *beta* (B.1.351) and *gamma* (P.1) *in vitro*, with 50% effective concentration (EC_{50}) estimates of 4.1 μM, 8.5 μM, 24.2 μM and 13.6 μM, respectively. A second study focusing on a combination of 10 μM stenoparib and 0.5 μM remdesivir resulted in over 90% inhibition of the *alpha* (B.1.1.7) variant, which is substantially greater than what was achieved with stenoparib or remdesivir alone at these concentrations.

30 **Importance**

31 The coronavirus disease (COVID-19) pandemic, caused by SARS-CoV-2, has caused
32 over 247 million infections and over 5 million deaths (1). Although protective vaccines are
33 available, the pandemic continues and both old and new SARS-CoV-2 variants may exhibit
34 degrees of resistance to vaccination. To date, only two antiviral drugs, remdesivir and
35 molnupiravir, or treatment with monoclonal antibodies, have been approved by the United
36 States Food and Drug Administration as COVID-19 therapies in certain situations. Additional
37 effective therapeutics are urgently needed. Here we describe the activity of a small molecule,
38 stenoparib, that effectively inhibits replication of SARS-CoV-2 wild-type and variant strains *in*
39 *vitro*. Stenoparib is an inhibitor of mammalian poly (ADP-ribose) polymerases (PARPs). A host-
40 targeting therapeutic like stenoparib could be a significant benefit for COVID-19 patients as a
41 standalone therapy, or especially as part of a combinatorial COVID-19 treatment strategy with
42 an antiviral drug such as remdesivir or molnupiravir.
43

44 **Observation**

45 Since the beginning of the COVID-19 pandemic, SARS-CoV-2 has mutated, which has
46 resulted in different variants of the virus. Only two antiviral drugs - remdesivir and molnupiravir,
47 or treatment with monoclonal antibodies, have been approved by the United States Food and
48 Drug Administration as COVID-19 therapies (2, 3). Remdesivir and molnupiravir are nucleoside
49 analogs that affect the activity of the RNA-dependent RNA polymerase (RdRp). After
50 incorporation into viral RNA, remdesivir stalls the RdRp during elongation (4), while molnupiravir
51 results in the incorporation of mutations that can be functionally deleterious (5). In contrast to
52 inhibitors that target viral replication, we recently published a study on the activity of a poly
53 (ADP-ribose) polymerase (PARP) inhibitor, stenoparib, also known as 2X-121, which inhibits
54 viral replication by affecting pathways of the host (6). ADP-ribosylation (ADPR) pathways may
55 have either anti- or pro-viral properties, and their importance in host-virus interactions is
56 becoming increasingly recognized (7). Unlike remdesivir, which inhibits viral replication
57 downstream of entry into the cell, stenoparib inhibits virus entry and post-entry processes (6).
58 Stenoparib inhibited the SARS-CoV-2 USA-WA1/2020 virus and the HCoV-NL63 human
59 seasonal respiratory coronavirus *in vitro*, exhibiting dose-dependent suppression of virus
60 multiplication and cell-cell spread in cell culture (6). Stenoparib exhibits a unique dual activity
61 against the PARP1, 2 and PARP5a, 5b (tankyrase 1, 2) enzymes, which are important
62 intermediates in the Wnt/β-catenin immune checkpoint (8, 9).

63 SARS-CoV-2 variants may carry mutations throughout the genome, particularly in the
64 sequence coding for the spike (S) protein. As a host-targeting therapeutic, we hypothesized that
65 the antiviral activity of stenoparib should be able to inhibit all variant strains. We explored the
66 activity of stenoparib against four additional SARS-CoV-2 variants of concern; SARS-CoV-2
67 Germany/BavPat1/2020 wild-type strain (wt) and variant strains (B.1.1.7 [*alpha*], B.1.351 [*beta*],
68 and P1 [*gamma*] – hereafter referred to using the Greek nomenclature). SARS-CoV-2 virus
69 variants were mixed with serial dilutions of compound and transferred to Vero E6 *Cercopithecus*

70 *aethiops* kidney cells, which were fixed and stained 20 hours (h) later with a SARS-CoV/SARS-
71 CoV-2 Nucleocapsid monoclonal antibody (Sino Biological) followed by a horseradish
72 peroxidase (HRP)-labeled Goat anti-Mouse IgG (Thermo Scientific) and TrueBlue substrate.
73 The 2 controls included on all assay plates were 1) infected and untreated cells and 2)
74 uninfected and untreated cells. The experiment was conducted in quadruplicate and the results
75 were calculated as the average fraction of wells that showed positive staining for the virus using
76 ViroSpot assay (10). Inhibition of virus replication by stenoparib was dose-dependent, with EC_{50}
77 ranging between 4.1 μM to 24.2 μM across the 4 variants tested (Fig. 1A). Interestingly, the
78 EC_{50} for the *beta* variant (24.2 μM) was 1.8- to 5.8-fold higher than for the wt, *alpha*, and
79 *gamma* variants (4.1, 8.5, and 13.6 μM, respectively). A similar phenomenon was noted for
80 remdesivir (Fig. 1B), where the EC_{50} for the *beta* variant (9.9 μM) was 2.0- to 2.6-fold higher
81 than for the wt, *alpha*, and *gamma* variants (3.8, 5.0, and 4.3 μM, respectively). According to a
82 recent report, the *beta* variant appears to exhibit a significantly reduced eclipse period and more
83 rapid replication *in vitro* (11), which would likely affect its dose response toward stenoparib and
84 remdesivir. The *beta* variant carries numerous changes to the S protein, several of which affect
85 the receptor binding domain and are also common to the *alpha* and *gamma* variants. In addition
86 to these changes, the *beta* variant carries mutations in the N protein and in the Nsp3 polyprotein
87 (ORF1a), which may be involved in ADPR following infection (12). Differential susceptibility to
88 ADPR may contribute to the altered replication kinetics of the *beta* variant, although this awaits
89 experimental validation.

90 In an additional set of experiments, we focused on the SARS-CoV-2 *alpha* variant. Vero
91 E6 cells were infected with the *alpha* variant using a multiplicity of infection of 0.1, and the
92 activity of stenoparib was assessed using the plaque reduction assay. Plaques are areas of
93 dead or destroyed cells and appear as small, clear regions in an infected cell monolayer after
94 fixation and staining with crystal violet. Following infection and treatment with an inhibitor, cells
95 were overlaid with low melting point agarose, fixed at 120 h post infection, stained with crystal

96 violet, and plaques were manually counted. The 3 control types were 1) infected and untreated
97 cells, 2) uninfected and untreated cells, and 3) infected cells treated with a combination of
98 camostat mesylate and E64d (CE), which are protease inhibitors that prevent spike protein
99 cleavage and virus entry into the cell (13). For the analysis shown in Fig. 2A and 2B, we
100 combined lower doses of stenoparib (2.5, 5.0, and 10 μM) with the previously reported 50%
101 effective concentration (EC_{50}) of remdesivir (0.5 μM) (6). In Fig. 2A and 2B, neither 10 μM
102 stenoparib nor 0.5 μM remdesivir achieved greater than a 50% reduction in plaquing efficiency
103 compared to the infected, untreated cells. When combined, however, synergy occurred as
104 plaque inhibition increased to over 90% - superior to what was achievable with either drug alone
105 ($P < 0.01$) at these doses. Notably, this was accomplished without significant cytotoxicity (Fig.
106 2C). Combinations of two or more drugs may lead to synergism through different mechanisms
107 of action, which has the potential benefit of reducing individual doses of each drug and
108 minimizing undesirable side effects.

109 Besides the known roles for the PARP1 and PARP2 enzymes in DNA repair (14, 15),
110 members of the PARP family have numerous additional functions (16). The 18 known human
111 PARPs appear to differentially affect viral replication; some exhibit proviral activity and others
112 exhibit antiviral roles (7, 17-21). In coronavirus, the N protein is mono (ADP) ribosylated
113 (MARylated) during infection. Stability of the N protein is critical for viral genome replication,
114 translation, packaging, and modulation of the host cell cycle (22). The N protein is the only
115 ADPR target definitively identified in coronavirus thus far (17), and the prevalence of this
116 modification across multiple coronavirus families suggests an important role in virus stability
117 (17). Despite this, the role of N protein MARylation, and of ADPR in general with regards to
118 coronavirus stability, is not well characterized. Possibly ADPR has a role in regulating virus
119 genome structure, similar to ADPR of histones or the adenovirus core proteins (23, 24). While
120 remdesivir and molnupiravir inhibit the viral replicon, stenoparib likely acts through multiple

121 targets. A combination of stenoparib and remdesivir or molnupiravir may be highly potent at

122 inhibiting SARS-family coronaviruses including SARS-CoV-2.

Acknowledgements

This research was supported by a grant from The Flinn Foundation, the Cowden Endowment for Microbiology, and an Arizona Board of Regents TRIF award. Core experiments were supported by service fees paid by Allarity Therapeutics.

Conflict of Interest Statement

SK is employed by and holds a financial interest in Allarity Therapeutics, which stands to potentially benefit from these results.

References

1. WHO. 2021. https://covid19.who.int/. Accessed 3 Nov 2021.
2. Prevention USCfDCa. 2020. Information for Clinicians on Investigational Therapeutics for Patients with COVID-19, *on* National Center for Immunization and Respiratory Diseases (NCIRD), Division of Viral Diseases. https://www.cdc.gov/coronavirus/2019-ncov/hcp/therapeutic-options.html. Accessed 16 Oct 2021.
3. Beigel JH, Tomashek KM, Dodd LE, Mehta AK, Zingman BS, Kalil AC, Hohmann E, Chu HY, Luetkemeyer A, Kline S, Lopez de Castilla D, Finberg RW, Dierberg K, Tapson V, Hsieh L, Patterson TF, Paredes R, Sweeney DA, Short WR, Touloumi G, Lye DC, Ohmagari N, Oh MD, Ruiz-Palacios GM, Benfield T, Fatkenheuer G, Kortepeter MG, Atmar RL, Creech CB, Lundgren J, Babiker AG, Pett S, Neaton JD, Burgess TH, Bonnett T, Green M, Makowski M, Osinusi A, Nayak S, Lane HC, Members A-SG. 2020. Remdesivir for the Treatment of Covid-19 - Final Report. N Engl J Med 383:1813-1826.
4. Kokic G, Hillen HS, Tegunov D, Dienemann C, Seitz F, Schmitzova J, Farnung L, Siewert A, Hobartner C, Cramer P. 2021. Mechanism of SARS-CoV-2 polymerase stalling by remdesivir. Nat Commun 12:279.
5. Kabinger F, Stiller C, Schmitzova J, Dienemann C, Kokic G, Hillen HS, Hobartner C, Cramer P. 2021. Mechanism of molnupiravir-induced SARS-CoV-2 mutagenesis. Nat Struct Mol Biol 28:740-746.
6. Stone NE, Jaramillo SA, Jones AN, Vazquez AJ, Martz M, Versluis LM, Raniere MO, Nunnally HE, Zarn KE, Nottingham R, Ng KR, Sahl JW, Wagner DM, Knudsen S, Settles EW, Keim P, French CT. 2021. Stenoparib, an Inhibitor of Cellular Poly(ADP-Ribose) Polymerase, Blocks Replication of the SARS-CoV-2 and HCoV-NL63 Human Coronaviruses In Vitro. mBio 12:e03495-20.
7. Kuny CV, Sullivan CS. 2016. Virus-Host Interactions and the ARTD/PARP Family of Enzymes. PLoS Pathog 12:e1005453.
8. McGonigle S, Chen Z, Wu J, Chang P, Kolber-Simonds D, Ackermann K, Twine NC, Shie JL, Miu JT, Huang KC, Moniz GA, Nomoto K. 2015. E7449: A dual inhibitor of PARP1/2 and tankyrase1/2 inhibits growth of DNA repair deficient tumors and antagonizes Wnt signaling. Oncotarget 6:41307-23.
9. Thorsell AG, Ekblad T, Karlberg T, Low M, Pinto AF, Tresaugues L, Moche M, Cohen MS, Schuler H. 2017. Structural Basis for Potency and Promiscuity in Poly(ADP-ribose) Polymerase (PARP) and Tankyrase Inhibitors. J Med Chem 60:1262-1271.
10. van Baalen CA, Jeeninga RE, Penders GH, van Gent B, van Beek R, Koopmans MP, Rimmelzwaan GF. 2017. ViroSpot microneutralization assay for antigenic characterization of human influenza viruses. Vaccine 35:46-52.
11. Pyke AT, Nair N, van den Hurk AF, Burtonclay P, Nguyen S, Barcelon J, Kistler C, Schlebusch S, McMahon J, Moore F. 2021. Replication Kinetics of B.1.351 and B.1.1.7 SARS-CoV-2 Variants of Concern Including Assessment of a B.1.1.7 Mutant Carrying a Defective ORF7a Gene. Viruses 13.
12. Lei J, Kusov Y, Hilgenfeld R. 2018. Nsp3 of coronaviruses: Structures and functions of a large multi-domain protein. Antiviral Res 149:58-74.
13. Hoffmann M, Kleine-Weber H, Schroeder S, Kruger N, Herrler T, Erichsen S, Schiergens TS, Herrler G, Wu NH, Nitsche A, Muller MA, Drosten C, Pohlmann S. 2020. SARS-CoV-2 Cell Entry Depends on ACE2 and TMPRSS2 and Is Blocked by a Clinically Proven Protease Inhibitor. Cell 181:271-280 e8.
14. Dziadkowiec KN, Gasiorowska E, Nowak-Markwitz E, Jankowska A. 2016. PARP inhibitors: review of mechanisms of action and BRCA1/2 mutation targeting. Prz Menopauzalny 15:215-219.

15. Ame JC, Rolli V, Schreiber V, Niedergang C, Apiou F, Decker P, Muller S, Hoger T, Menissier-de Murcia J, de Murcia G. 1999. PARP-2, A novel mammalian DNA damage-dependent poly(ADP-ribose) polymerase. J Biol Chem 274:17860-8.
16. Gupte R, Liu Z, Kraus WL. 2017. PARPs and ADP-ribosylation: recent advances linking molecular functions to biological outcomes. Genes & development 31:101-126.
17. Grunewald ME, Fehr AR, Athmer J, Perlman S. 2018. The coronavirus nucleocapsid protein is ADP-ribosylated. Virology 517:62-68.
18. Grunewald ME, Chen Y, Kuny C, Maejima T, Lease R, Ferraris D, Aikawa M, Sullivan CS, Perlman S, Fehr AR. 2019. The coronavirus macrodomain is required to prevent PARP-mediated inhibition of virus replication and enhancement of IFN expression. PLoS Pathog 15:e1007756.
19. Li L, Zhao H, Liu P, Li C, Quanquin N, Ji X, Sun N, Du P, Qin C-F, Lu N, Cheng G. 2018. PARP12 suppresses Zika virus infection through PARP-dependent degradation of NS1 and NS3 viral proteins. Science signaling 11:eaas9332.
20. Atasheva S, Frolova EI, Frolov I. 2014. Interferon-stimulated poly(ADP-Ribose) polymerases are potent inhibitors of cellular translation and virus replication. Journal of virology 88:2116-2130.
21. Westera L, Jennings AM, Maamary J, Schwemmle M, Garcia-Sastre A, Bortz E. 2019. Poly-ADP Ribosyl Polymerase 1 (PARP1) Regulates Influenza A Virus Polymerase. Adv Virol 2019:8512363.
22. McBride R, van Zyl M, Fielding BC. 2014. The coronavirus nucleocapsid is a multifunctional protein. Viruses 6:2991-3018.
23. Déry CV, de Murcia G, Lamarre D, Morin N, Poirier GG, Weber J. 1986. Possible role of ADP-ribosylation of adenovirus core proteins in virus infection. Virus Research 4:313-329.
24. Strickfaden H, McDonald D, Kruhlak MJ, Haince J-F, Th'ng JPH, Rouleau M, Ishibashi T, Corry GN, Ausio J, Underhill DA, Poirier GG, Hendzel MJ. 2016. Poly(ADP-ribosyl)ation-dependent Transient Chromatin Decondensation and Histone Displacement following Laser Microirradiation*. Journal of Biological Chemistry 291:1789-1802.

211 **Figures**

212

213 **Figure 1.** Dose-response curves for stenoparib and remdesivir on SARS-CoV-2 variants. **A.**
214 stenoparib. **B.** remdesivir. Vero E6 cells (ATCC CRL-1586) were infected for 20 hours with
215 SARS-CoV-2 wild type (wt) or the indicated variants in the presence or absence of stenoparib or
216 remdesivir as indicated. Results are the average fraction of quadruplicate wells that exhibited
217 positive staining for SARS-CoV-2 (y-axis) vs. the concentration of the inhibitors (x-axis). These
218 data were used to estimate the EC_{50} of stenoparib and remdesivir. The EC_{50} values were
219 approximated with the aid of the online calculator from AAT Bioquest ("Quest Graph™ EC_{50}
220 Calculator." AAT Bioquest, Inc, 26 Oct. 2020, https://www.aatbio.com/tools/ec50-calculator).
221 Viruses; wild-type (wt): BetaCoV/Munich/BavPat1/2020, European Virus Archive Global. *Alpha*:
222 USA/CA_CDC_5574/2020, BEI Resources, Cat# NR-54011. *Beta*: hCoV-19/South
223 Africa/KRISP-K005325/2020, BEI Resources. *Gamma*: hCoV-19/Japan/TY7-503/2021 (Brazil
224 P.1), BEI Resources.

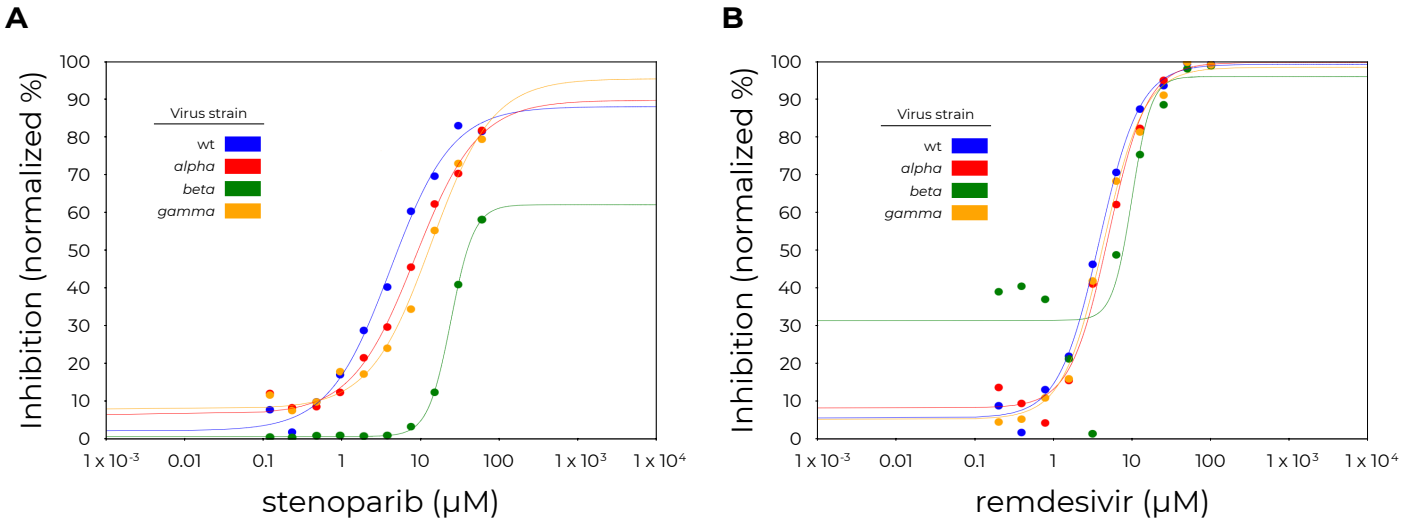

225 **Figure 2.** Activity of stenoparib and remdesivir on the *alpha* (B.1.1.7) variant. **A.** Virus Plaque
226 assays. Vero E6 cells (ATCC CRL-1586) were infected for 2 hours with SARS-CoV-2 *alpha*
227 (USA/CA_CDC_5574/2020, BEI Resources, Cat# NR-54011), washed, and overlaid with low-
228 melting temp agarose/MEM with or without stenoparib and/or remdesivir at the concentrations
229 indicated. The cell monolayers were fixed with 4% paraformaldehyde and stained with 0.1%
230 crystal violet prior to manual counting of clear plaques. The experiment was performed using
231 technical triplicates, and error bars represent the standard deviation of three independent
232 experiments. Statistical analysis was performed using the Student's unpaired t-test. * $P < 0.05$,
233 ** $P < 0.01$ applies where indicated. **B.** Photographs of plate wells after crystal violet staining.
234 Labels indicate the concentrations of stenoparib or remdesivir. Abbreviations: S = stenoparib, R
235 = remdesivir at the concentrations indicated (e.g. S2.5 / R0.5 = stenoparib 2.5 μM, remdesivir
236 0.5 μM, etc.). **C.** Cytotoxicity measurements performed by the lactate dehydrogenase release
237 assay (Promega Cytotox 96) 48 hours after infection. Inhibitors stenoparib or remdesivir were
238 used at the indicated concentrations (x-axis). The assays were performed according to the
239 manufacturer's recommendations. Results from drug treatments were normalized to the fraction
240 of maximum cytotoxicity (percent cytotoxicity; y-axis) achieved by detergent lysis of cells. The
241 experiment was performed using technical triplicates, and error bars represent the standard
242 deviation of three independent experiments.

243

A

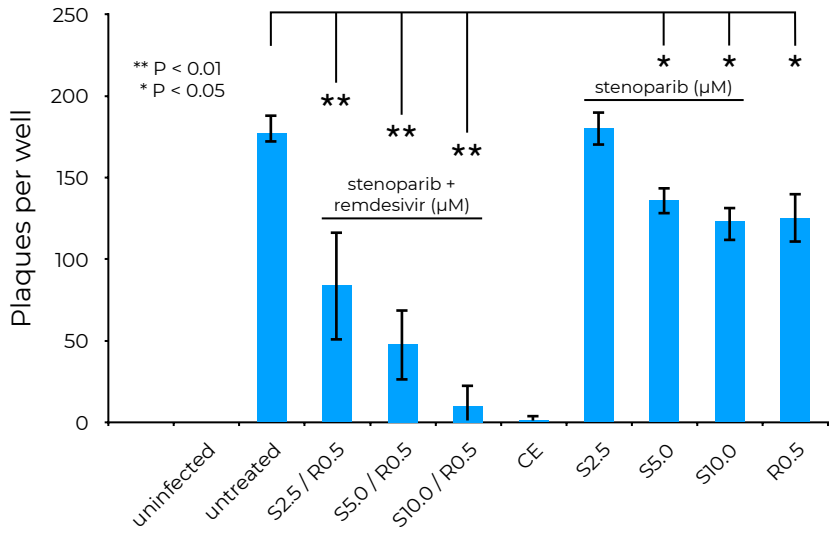
** P < 0.01
* P < 0.05
Plaques per well
250
200
150
100
50
0
stenoparib + remdesivir (μM)
stenoparib (μM)
uninfected
untreated
S2.5 / R0.5
S5.0 / R0.5
S10.0 / R0.5
CE
S2.5
S5.0
S10.0
R0.5

B

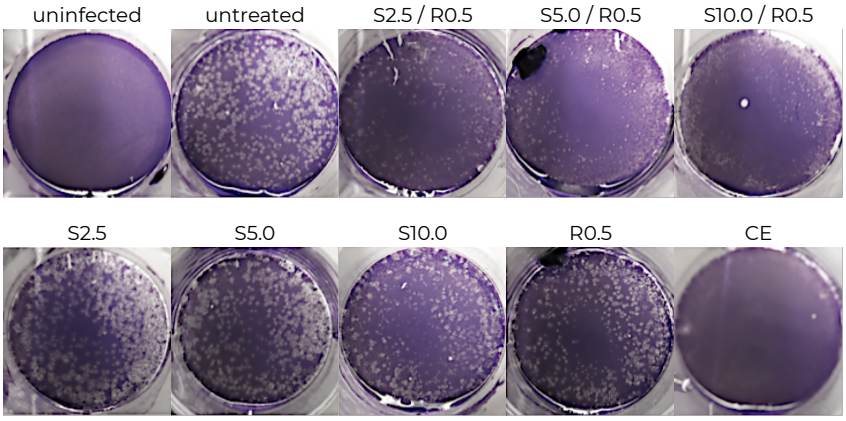
uninfected
untreated
S2.5 / R0.5
S5.0 / R0.5
S10.0 / R0.5
S2.5
S5.0
S10.0
R0.5
CE

C

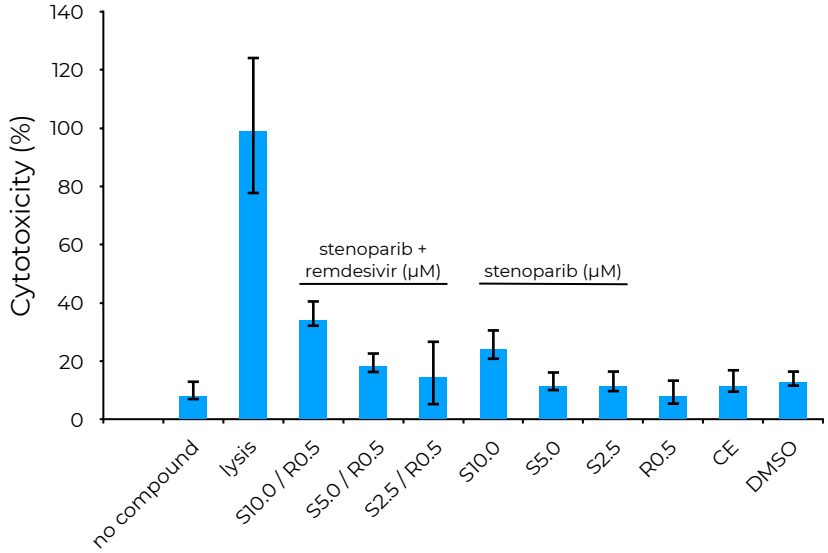
Cytotoxicity (%)
140
120
100
80
60
40
20
0
stenoparib + remdesivir (μM)
stenoparib (μM)
no compound
lysis
S10.0 / R0.5
S5.0 / R0.5
S2.5 / R0.5
S10.0
S5.0
S2.5
R0.5
CE
DMSO